Rapid Communications

Extracting free-space observables from trapped interacting clusters

Xilin Zhang *

Department of Physics, The Ohio State University, Columbus, Ohio 43210, USA
and Physics Department, University of Washington, Seattle, Washington 98195, USA

(Received 24 June 2019; revised manuscript received 4 September 2019; accepted 27 April 2020; published 14 May 2020)

The energy spectrum of two short-range interacting particles in a harmonic potential trap has previously been related to free-space scattering phase shifts. But the existing formula for systems with a nonzero interaction range is exact only in the limit of an infinitely shallow trap. Here I provide a systematically improved formula—describing the low-energy dynamics—that enables the use of finite traps. This paves the way for extracting nuclear scattering phase shifts from *ab initio* nuclear many-body structure calculations, a long-sought goal in nuclear physics. The derivation establishes effective field theory as a powerful framework for studying the connection between structure information of a trapped system (with two or more subclusters) and continuum physics in the fields of both nuclear and condensed-matter physics.

DOI: 10.1103/PhysRevC.101.051602

I. INTRODUCTION

Nuclear experiments at low energy can not manipulate many-body systems to the extent possible in condensed-matter or cold-atom experiments. However, with progress in many-body methods [1–5] and increasing computing power (and quantum computers [6]), one can start manipulating nuclear systems *computationally*. Here, I show how trapping two clusters at low energy in a harmonic potential well tells us about their free-space scattering through a formula connecting low-energy phase shifts with the confined spectrum. In this approach the trap compacts the system and reduces the required degrees of freedom enough to allow controlled *ab initio* calculations, as will be demonstrated elsewhere. (See, e.g., Refs. [7–10] for other *ab initio* approaches of computing light-nucleus scatterings.)

A formula for particles in a harmonic-potential trap was derived in Ref. [11] and later generalized to include the full energy dependence of the phase shift (besides the scattering length term in Ref. [11]) and for partial waves beyond s wave [12–20]. The result for angular momentum ℓ [17,18,21] (called the BERW formula here) is

$$p^{2\ell+1}\cot\delta_\ell(E) = (-)^{\ell+1}(4M_{\rm R}\omega)^{\ell+\frac{1}{2}}\frac{\Gamma\left(\frac{3}{4}+\frac{\ell}{2}-\frac{E}{2\omega}\right)}{\Gamma\left(\frac{1}{4}-\frac{\ell}{2}-\frac{E}{2\omega}\right)}. \quad (1)$$

This holds at the eigenenergies $E \equiv p^2/2M_{\rm R}$—with the center-of-mass (CM) energy subtracted—in a trap where each particle experiences a potential $\omega^2\boldsymbol{r}^2/2$ times its mass; $M_{\rm R}$ is the reduced mass and δ_ℓ is the phase shift. Equation (1) is analogous to the Luscher formula [22,23] that is widely applied in lattice quantum chromodynamics (for a system on a space-time torus).

References [21,24] have used Eq. (1) to extract nuclear scattering from *ab initio* spectrum calculations. However, away from the infinitely-shallow-trap limit (i.e., for $\omega \neq 0$), Eq. (1) does not capture the external potential's modifications to the interaction at short distances. To illustrate the impact on extracting phase shifts, I use a two-body potential model [25] designed for describing neutron-α scattering [see the Supplemental Materials (SM) [26] for details]. Figure 1(a) shows $3/2^-$ p-wave phase shifts extracted by using Eq. (1) at the eigenenergies with $\omega = 3, 4, 6, 9, 16$ MeV (typical values applicable in *ab initio* calculations): they fail to align on a smooth curve and systematically deviate from the exact curve [21].

Here, I remedy the BERW formula by using pionless effective field theory (EFT) [27–29], which enables low-energy dynamics to be studied without specifying the details of the short-distance physics (e.g., potential or cluster structure and excitation). This EFT was used to rederive and generalize the Luscher formula [23,30]. The improved formula for a harmonic trap is

$$\sum_{i,j=0}^{\infty} C_{i,j}(M_{\rm R}\omega)^{2i}p^{2j} = (-)^{\ell+1}(4M_{\rm R}\omega)^{\ell+\frac{1}{2}}\frac{\Gamma\left(\frac{3}{4}+\frac{\ell}{2}-\frac{E}{2\omega}\right)}{\Gamma\left(\frac{1}{4}-\frac{\ell}{2}-\frac{E}{2\omega}\right)},$$

$$p^{2\ell+1}\cot\delta_\ell(E) = \sum_{j=0}^{\infty} C_{i=0,j}p^{2j}. \quad (2)$$

The constants $C_{i,j}$ depend implicitly on ℓ but are independent of ω and p; they are dimensionful and scale as proper powers of a high-momentum scale M_H (as dictated by, e.g., the cluster excitations), unless there is fine tuning. When $\sqrt{M_{\rm R}\omega}$ and p are smaller than M_H, the series sum converges and thus can be truncated with a controlled error. However, outside the convergence domain, where the details of the finite-range interaction and its interplay with the trap potential are being probed, the

*zhang.10038@osu.edu

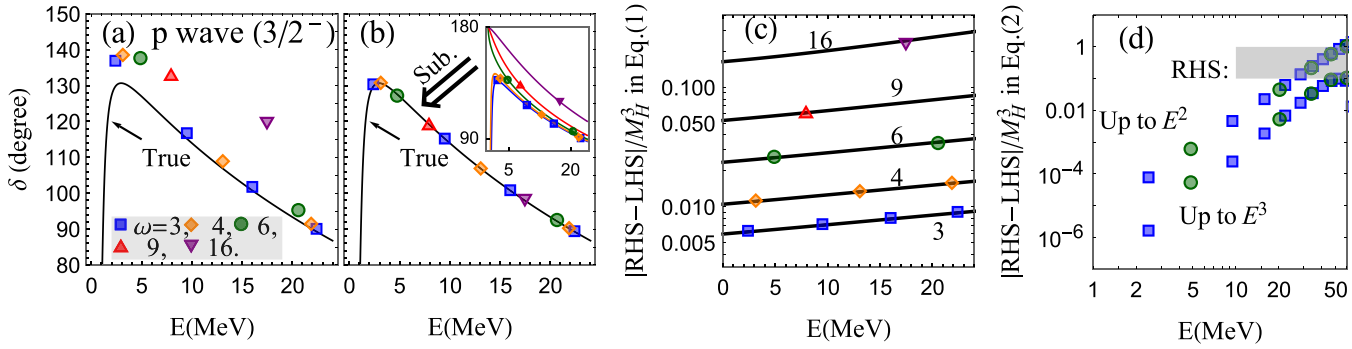

FIG. 1. (a) The n-α p-wave scattering phase shifts extracted using Eq. (1) at the ω-dependent eigenenergies. The "True" curves are the exact phase shifts. (b) After subtracting ω-dependent pieces from *generalized* ERE curves (inset), the extractions from Eq. (2) lie on the "True" curve. (c) Discrepancies of Eq. (1) at those eigenenergies. The curves plot the summation of the $C_{i\neq 0,j}$ terms on the LHS of Eq. (2). (d) Discrepancies of Eq. (2) at those eigenenergies with two different truncations on the i and j indices in its LHS: "Up to E^2" and "E^3". The shaded area is the range of the RHS of Eq. (2) ($E \geqslant 10$ MeV). Note that all panels use the legend from panel (a).

series expansion becomes infeasible. It is also worth noting that, in the case of *physically* zero-range interactions (i.e., $M_H \to \infty$), the $C_{i\neq 0,j}$ terms, which capture the trap-induced modifications, would vanish, and Eq. (2) becomes equivalent to Eq. (1).

To infer the phase shifts from Eq. (2) given the eigenenergies, the $C_{i\neq 0,j}$ terms must be simultaneously calibrated with the $C_{0,j}$. The latter determine the free-space phase shifts via the effective range expansion (ERE) [27,29]. Knowing the full potential in the n-α model, one can fix $C_{i,j}$ (see the SM [26]) and generate Fig. 1(b): the inset shows that the phase shifts extracted from Eq. (1) for a given ω sit on a curve parametrized by a *generalized* ERE, in which the jth-order coefficient is given by $\sum_{i=0} C_{i,j}(M_{\rm R}\omega)^{2i}$. After subtracting the trap-induced modifications, the extracted phase shifts agree with the "True" curve.

The essence of Eq. (2), that the trap-induced modifications can be parametrized by using a Taylor expansion in the ω^2 and p^2 variables, can be seen in Fig. 1(c). The symbols show the differences between the right-hand-side (RHS) and left-hand-side (LHS) in Eq. (1)—scaled by M_H^{-3}—at the ω-dependent eigenenergies, while the solid lines plot the summation of the $C_{i\neq 0,j}$ terms on the LHS of Eq. (2) with $i \leqslant 2$ and $0 \leqslant j \leqslant 3$. Indeed, they interpolate those symbols. Of course, outside the convergence domain, the series expansion would fail, as shown in Fig. 1(d). The differences between the two sides of Eq. (2), based on two series truncations ($j \leqslant 3$ for "Up to E^3" and $j \leqslant 2$ for "Up to E^2," and $i \leqslant 2$ in both cases), are plotted against a large range of eigenenergies. The truncation errors behave as the leading terms left out of the summation in the low-energy region, but then increase to 100% when the symbols reach the shaded region, indicating the range of the RHS of Eq. (2); this also suggests that the breakdown scale for E is between 20 and 40 MeV. (See the SM [26] for more details on series convergence.)

To extract nuclear phase shifts (or $C_{i,j}$s) from *ab initio* spectra, Eq. (2) will play a crucial role because *ab initio* calculations, developed for computing compact nuclei, have uncontrolled errors when $\omega \to 0$. To illustrate Eq. (2), two models are used in the SM [26]: a hard-sphere potential model is solved exactly, while the n-α model is studied numerically. The rest of the paper is devoted to the derivation of Eq. (2), emphasizing a new set of interaction vertices between the external potential (or background field) and trapped particles, and renormalization.

II. DERIVATION THROUGH EFFECTIVE FIELD THEORY

I start by constructing an EFT Lagrangian for two spin-0 particles—for simplicity—in the ℓth partial wave, with a harmonic potential coupled to each particle. The framework is valid at low energies, where the details of the short-distance physics and its interplay with the trap are not resolved. I follow the conventions of Ref. [31]. Let $c(x)$ and $n(x)$ be particle fields with masses $M_{\rm c}$ and $M_{\rm n}$ (c^* and n^* are the complex conjugations), while ϕ_{m_ℓ} is the so-called dimer field [28–30,32–35] with spin ℓ, projection m_ℓ, and mass $M_{nc} = M_{\rm n} + M_{\rm c}$ [$\phi^{\dagger m_\ell} \equiv (\phi_{m_\ell})^*$]. The dimer ϕ couples to n-c and represents the compound system. The background field $\mathscr{B}(x)$ is $m\omega^2\boldsymbol{x}^2/2$ in the lab frame with m as a reference mass. The ϕ propagator—and the related self-energy corrections due to n-c multiple scattering—will be the central piece in the derivation: in free space it is directly related to the n-c scattering T matrix, while in the trap its poles give the system's spectrum.

The Lagrangian is $\mathscr{L}_0 + \mathscr{L}_I$, where

$$\mathscr{L}_0 = (c^*, \quad n^*, \quad \sigma_\ell \phi^{\dagger m_\ell}) \,\mathrm{diag}\left(i\tilde{\partial}_t + \frac{\boldsymbol{\partial}^2}{2M_c} + \Delta_c, i\tilde{\partial}_t + \frac{\boldsymbol{\partial}^2}{2M_n} + \Delta_n, i\tilde{\partial}_t + \frac{\boldsymbol{\partial}^2}{2M_{nc}} + \Delta_\ell\right)(c, \quad n, \quad \phi_{m_\ell})^T, \tag{3}$$

$$\mathscr{L}_I = g_\ell \phi^{\dagger m_\ell} c[V^{\otimes \ell}]_{m_\ell} n + \text{c.c.} - \phi^{\dagger m_\ell}\left[d^{(\ell)}_{j\geqslant 2}\left(i\tilde{\partial}_t + \frac{\boldsymbol{\partial}^2}{2M_{nc}}\right)^j + d^{(\ell)}_{j\geqslant 0,k\geqslant 1}\left(i\tilde{\partial}_t + \frac{\boldsymbol{\partial}^2}{2M_{nc}}\right)^j \left(\frac{M_{\rm R}^2}{3m}\boldsymbol{\partial}^2\mathscr{B}\right)^k\right]\phi_{m_\ell}. \tag{4}$$

Here, c.c. is for complex conjugate. The building blocks of $\mathscr{L}_{0,I}$ are invariant under Galilean transformations, including rotation, translation, and boost. (A relevant discussion on Galilean invariance in EFT can be found, e.g., in Ref. [36].) In both Lagrangians for $\psi = n$, c, or ϕ, the $\psi^*[i\tilde{\partial}_t + \boldsymbol{\partial}^2/(2M_\psi)]\psi$ structures with $i\tilde{\partial}_t \equiv i\partial_t - M_\psi\mathscr{B}(x)/m$ are ψ's internal energies (i.e., total energies with kinetic and external potential energies subtracted), and therefore Galilean invariant.

The g_ℓ coupling in $\mathscr{L}_I$ uses n-c's relative velocity $\boldsymbol{V}$, while $V^{\otimes\ell}$ denotes a rank-ℓ operator composed of ℓ copies of $\boldsymbol{V}$ normalized such that when $m_\ell = +\ell$, $[V^{\otimes\ell}]_{m_\ell} = [(V^{+1})^\ell]^*$ with $V^{+1} \equiv -(V^x + iV^y)/\sqrt{2}$. This term means $\phi^{\dagger m_\ell}$ is coupled to an n-c configuration having ℓ and m_ℓ as its relative angular quantum numbers. The m_ℓ indices are implicitly summed up so that this term is a scalar. (In general, the spin and vector indices need to be properly contracted to form scalars.) In addition, both $\boldsymbol{V}$ and spins are invariant under translation and boost, and thus the g_ℓ coupling preserves Galilean invariance. Note that repeated indices in the Lagrangian [and in Eqs. (6), (8), and (9)] are implicitly summed with specified ranges.

It should be mentioned that the interactions in $\mathscr{L}_0$ and $\mathscr{L}_I$ with the external potential turned off follow closely previous works using a dimer-field approach [28–30,32–35]: σ_ℓ ($=\pm1$), Δ_ℓ, g_ℓ, and $d_j^{(\ell)}$ together reproduce the ERE [see Eq. (6) and Refs. [30,33]]. This approach is equivalent [28,32,35] to the EFTs without dimer fields (see further discussion in Sec. III).

The $d^{(\ell)}_{j\geqslant0,k\geqslant1}$ terms are also Galilean invariant, considering that the external potential $\mathscr{B}$ is a scalar field. However, their specific structures are severely constrained by a unique property of a harmonic potential: the CM of a multiparticle system is decoupled from its internal dynamics [37]. (It can be understood based on that the external force on the multiparticle's CM depends only on CM's location in the harmonic potential well, i.e., not affected by any other degrees of freedom.) In these couplings with $M_{\rm R}^2\boldsymbol{\partial}^2\mathscr{B}/(3m) = M_{\rm R}^2\omega^2$, $\boldsymbol{\partial}^2$ ensures that they only shift the system's energy by $\boldsymbol{r}$-independent but ω^2-dependent functions so that the CM behaves as a free particle in traps, i.e., decoupled from internal dynamics.

Besides powers of $\boldsymbol{\partial}^2\mathscr{B}$, the other possible scalar objects built of $\mathscr{B}$ include (1) $\mathscr{B}^2$, $\mathscr{B}^3$, ...(2) $(\boldsymbol{\partial}\mathscr{B})^4$, $(\boldsymbol{\partial}\mathscr{B})^6$, ...[$(\boldsymbol{\partial}\mathscr{B})^2$ is proportional to $\mathscr{B}$], and (3) products of (1) and (2). (Derivatives higher than $\boldsymbol{\partial}^2$ applied on $\mathscr{B}$ would give zero and therefore are not relevant here.) They would induce external potentials with powers of $\boldsymbol{r}^2$ higher than unity. Copies of $\boldsymbol{\partial}\mathscr{B}$ can also be used to construct tensor (vector) objects, which create anisotropic external potentials that need to be coupled to particles' momenta or spins. As the result, the new scalar and tensor objects and their products would break the CM–internal-dynamics decoupling if they are present in any interaction terms with particles.

In principle, $\mathscr{B}$ can be coupled to the ϕ^*nc operators (e.g., the g_ℓ term), which again must take the form of $(\boldsymbol{\partial}^2\mathscr{B})^{1,2,\cdots}$. However, these terms can be eliminated by rescaling the ϕ field by $1 + \#(M_{\rm R}\omega)^2 + \cdots$ [38]. Since the rescaling-induced terms are already present as $d_{j,k}^{(\ell)}$ couplings in $\mathscr{L}_I$, the trap modification to g_ℓ is not included.

Lastly, in the free space, defining energy relative to the n-c threshold sets $\Delta_c = \Delta_n = 0$. Both are modified by $\mathscr{B}$ through "polarization" effects as Δ_ℓ by $d^{(\ell)}_{j=0,k}$ couplings, but they only affect the energy references in traps and for simplicity are not shown here.

To compute the propagator of the dimer ϕ, its self-energy correction due to n-c multiple scattering needs to be included. A cutoff on momentum is applied to regularize loops in free space, while in traps the cutoff is applied on the virtual excitation energy [27]. (However, for fine-tuned systems other schemes would be preferred, e.g., power divergence subtraction [39].) Within time-independent perturbation theory [31], the one-loop self-energy bubble diagram in free space is $(2\pi)^3\delta(\boldsymbol{P}-\boldsymbol{P}')\delta^{m_\ell}_{m'_\ell}\Sigma(E_L,\boldsymbol{P}) \equiv \langle\phi^{m'_\ell}_{\boldsymbol{P}'}|H_{g_\ell}(E_L - H_0 + i0^+)^{-1}H_{g_\ell}|\phi^{m_\ell}_{\boldsymbol{P}}\rangle$. H_0 and H_{g_ℓ} are the Hamiltonians derived from $\mathscr{L}_0$ and the g_ℓ term in $\mathscr{L}_I$, respectively [31]. Both states are plane waves, with $\boldsymbol{P}$, $\boldsymbol{P}'$, E_L, m_ℓ, and m'_ℓ as ϕ's momenta and energy in the lab frame, and its spin projections. (The relationships between Feynman diagrams and the matrix elements defined here and below can be found in Ref. [31].) One then obtains

$$\begin{aligned}\Sigma(E) &= \frac{\mathscr{A}_\ell}{\pi}\int_0^{T_\Lambda} dT_q \frac{(2M_{\rm R}T_q)^{\ell+\frac{1}{2}}}{E - T_q + i0^+} \\ &= -\mathscr{A}_\ell\left[ip^{2\ell+1} + \sum_{j=0}^{+\infty} L_{\ell,j}(\Lambda)p^{2j}\right], \\ \mathscr{A}_\ell &\equiv \frac{g_\ell^2}{M_{\rm R}^{2\ell-1}}\frac{2^{\ell-1}\ell!^2}{\pi(2\ell+1)!}, \quad L_{\ell,j}(\Lambda) \equiv \frac{2\Lambda^{2\ell-2j+1}}{\pi(2\ell-2j+1)}.\end{aligned} \tag{5}$$

$p \equiv [2M_{\rm R}(E+i0^+)]^{1/2}$, $T_q \equiv \boldsymbol{q}^2/(2M_{\rm R})$, Λ is the cutoff on $|\boldsymbol{q}|$, and $T_\Lambda \equiv \Lambda^2/(2M_{\rm R})$. $E \equiv E_L - \boldsymbol{P}^2/(2M_{nc})$ is the energy in the CM frame. Note that $L_{\ell,j>\ell}(\Lambda) \to 0$ as $\Lambda \to \infty$.

The fully dressed free-space ϕ propagator, which is defined through $(2\pi)^3\delta(\boldsymbol{P}-\boldsymbol{P}')\delta^{m_\ell}_{m'_\ell}D(E_L,\boldsymbol{P}) \equiv \langle\phi^{m'_\ell}_{\boldsymbol{P}'}|[E_L - (H_0+H_I) + i0^+]^{-1}|\phi^{m_\ell}_{\boldsymbol{P}}\rangle$, with H_I from $\mathscr{L}_I$, can be computed by summing the self-energy-insertion diagrams due to Σ and the $d_j^{(\ell)}$ vertices, yielding

$$\begin{aligned}D &= \frac{1}{\sigma_\ell(E+\Delta_\ell) - d_j^{(\ell)}E^j - \Sigma} \\ &= \frac{-\mathscr{A}_\ell^{-1}}{p^{2\ell+1}[\cot\delta_\ell - i]}, \\ \text{with } p^{2\ell+1}\cot\delta_\ell &= \sum_{j=0}^{\infty} C_{0,j}p^{2j}, \text{ and} \\ C_{0,j} &= \frac{\mathscr{A}_\ell^{-1}}{(2M_{\rm R})^j}\left\{-\sigma_\ell\Delta_\ell, -\sigma_\ell, d_2^{(\ell)}, d_3^{(\ell)}, \dots\right\}_j \\ &\quad -L_{\ell,j}(\Lambda).\end{aligned} \tag{6}$$

D is related to δ_ℓ through the scattering T matrix, which is computed by multiplying D with two g_ℓ vertices [31]. The range of the index in $d_j^{(\ell)}$ in the implicit sum is fixed in $\mathscr{L}_I$, and in the $C_{0,j}$ definition $\{\ldots\}_j$ is the jth component of the list and j is not summed.

Now let us turn to the trapped system. Based on $\mathscr{L}_0$, one can expand n, c, and ϕ fields using their corresponding harmonic-oscillator wave functions [18]. Again note that the g_ℓ coupling only picks up the n-c configuration whose *total* angular momentum and projection equal those of the CM motion (i.e., ϕ) and whose *relative* angular momentum and projection equal the ϕ's spin and projection (ℓ and m_ℓ). Thus the matrix element between ϕ's eigenstates in a trap for defining its self-energy becomes $\delta^{N'_\phi}_{\boldsymbol{N}_\phi}\delta^{m'_\ell}_{m_\ell}\Sigma_\omega(E) \equiv \langle\phi^{m'_\ell}_{\boldsymbol{N}'_\phi}|H_{g_\ell}(E_L - H_0)^{-1}H_{g_\ell}|\phi^{m_\ell}_{\boldsymbol{N}_\phi}\rangle$ (note the absence of $i0^+$ in the Green's function), with

$$\begin{aligned}\Sigma_\omega(E) &= \frac{g_\ell^2}{M_{\rm R}^{2\ell}}\frac{(2\ell+1)!}{2^{\ell+2}\pi}\sum_{n=0}^{n_\Lambda}\frac{(\bar{R}^{(r)}_{n,\ell}(0))^2}{E-E^{(r)}_{n,\ell}}\\ &= \frac{\mathscr{A}_\ell}{\pi}(4M_{\rm R}\omega)^{\ell+\frac{1}{2}}\sum_{n=0}^{n_\Lambda} f_\ell(z_E,n),\\ f_\ell(z_E,n) &\equiv \frac{\Gamma\left(n+\ell+\frac{3}{2}\right)/\Gamma(n+1)}{z_E-\left(n+\frac{\ell}{2}+\frac{3}{4}\right)}.\end{aligned} \tag{7}$$

Here $z_E \equiv E/(2\omega)$ and the relative energy $E \equiv E_L - E^{(\phi)}_{\boldsymbol{N}_\phi}$, with $E^{(\phi)}_{\boldsymbol{N}_\phi} = (2N_\phi + \ell_\phi + \frac{3}{2})\omega$ as the CM energy. If Δ_c and Δ_n receive trap-dependent "polarization" corrections, these corrections also need to be subtracted in defining E. In the derivation, a unitary transformation between n and c single-particle and CM and relative motion eigenmodes has been used.

Summing over the quantum numbers associated with the intermediate state's CM motion gives rise to the $\delta^{N'_\phi}_{\boldsymbol{N}_\phi}$ factor in defining Σ_ω, since the CM's decoupling property is preserved and thus so is $\boldsymbol{N}_\phi$. For the relative dynamics, $\bar{R}^{(r)}_{n,\ell}$ is part of the eigenmode function $R^{(r)}_{N_r}$ [18]: $R^{(r)}_{N_r}(\boldsymbol{r}) \equiv \bar{R}^{(r)}_{n,\ell}(r)\, r^\ell Y_{\ell m_\ell}(\hat{r})$. N_r has n, ℓ for its radial excitation and angular momentum, and $E^{(r)}_{n,\ell} = (2n+\ell+\frac{3}{2})\omega$. A cutoff on n is used to regularize the theory in a trap, which is in parallel with the regularization used in Eq. (5).

The ϕ propagator in the trap, defined as $D_\omega(E)\delta^{N'_\phi}_{\boldsymbol{N}_\phi}\delta^{m'_\ell}_{m_\ell}$, can be computed by summing up all self-energy insertion diagrams, including insertions of Σ_ω and those of the $d_j^{(\ell)}$ and $d_{j,k}^{(\ell)}$ vertices. One gets

$$\begin{aligned}D_\omega &= \frac{1}{\sigma_\ell(E+\Delta_\ell) - d_j^{(\ell)}E^j - \Sigma_\omega(E) - d_{j,k}^{(\ell)}E^j(M_{\rm R}\omega)^{2k}}\\ &= \frac{(-)\mathscr{A}_\ell^{-1}}{p^{2\ell+1}\cot\delta_\ell + \frac{1}{\mathscr{A}_\ell}\left[\Sigma_\omega(E) - \mathscr{P}\Sigma(E) + d_{j,k}^{(\ell)}E^j(M_{\rm R}\omega)^{2k}\right]}.\end{aligned} \tag{8}$$

In the second step, the principal value of the free-space self-energy $\mathscr{P}\Sigma$ is added and subtracted. Thus, the quantization condition can be derived by setting the denominator in Eq. (8) to zero:

$$p^{2\ell+1}\cot\delta_\ell(E) + \frac{d_{j,k}^{(\ell)}}{\mathscr{A}_\ell}E^j(M_{\rm R}\omega)^{2k} = \frac{\mathscr{P}\Sigma(E) - \Sigma_\omega(E)}{\mathscr{A}_\ell}. \tag{9}$$

There exists a special relation between Λ (or $\bar{T}_\Lambda \equiv T_\Lambda/\omega$) and n_Λ such that the divergences in Σ and Σ_ω cancel in Eq. (9), and thus $d_{j,k}^{(\ell)}$ are finite. For s wave, $\bar{T}_\Lambda = 2n_\Lambda[1 + O(n_\Lambda^{-1})]$, but for p wave the n_Λ^{-1}-order term needs to be specified: $\bar{T}_\Lambda = 2n_\Lambda[1 + \frac{7}{4}n_\Lambda^{-1} + O(n_\Lambda^{-2})]$; for d wave another higher-order term needs to be specified: $\bar{T}_\Lambda = 2n_\Lambda[1 + \frac{9}{4}n_\Lambda^{-1} - \frac{37}{32}n_\Lambda^{-2} + O(n_\Lambda^{-3})]$; for even larger ℓ, more terms need to be specified accordingly. Details on the renormalization can be found in the SM [26]. However, the above n_Λ-Λ relations should be considered as a specific scheme; any alternative ones would need to ensure that the divergences on the RHS of Eq. (9) can be absorbed by the $d_{j,k}^{(l)}$ terms on the left side so that phase shifts are cutoff-independent and the CM-decoupling property is not violated.

The right side of Eq. (9) in this scheme then becomes

$$\begin{aligned}&-\frac{1}{\pi}(4M_{\rm R}\omega)^{\ell+\frac{1}{2}}\left[\sum_{n=0}^{n_\Lambda} f_\ell(z_E,n) + \pi\sum_{j=0}^{\ell} z_E^j L_{l,j}\left(\sqrt{\tfrac{\bar{T}_\Lambda}{2}}\right)\right]\\ &\equiv -\frac{1}{\pi}(4M_{\rm R}\omega)^{\ell+\frac{1}{2}}\sum_{n=0}^{(\mathscr{R})} f_\ell(z_E,n),\end{aligned} \tag{10}$$

with "$(\mathscr{R})$" labeling the renormalized series sum with $n_\Lambda \to +\infty$. To finish the derivation, this identity is needed:

$$\sum_{n=0}^{(\mathscr{R})} f_\ell(z,n) = (-)^\ell\pi\,\frac{\Gamma\left(\frac{\ell}{2}+\frac{3}{4}-z\right)}{\Gamma\left(\frac{1}{4}-\frac{\ell}{2}-z\right)}, \tag{11}$$

which holds in the entire complex z plane (both sides have the same poles and residues, see the proof in the SM [26]). By redefining $d_{j,i}^{(\ell)} \equiv \mathscr{A}_\ell(2M_{\rm R})^j C_{i,j}$ in Eq. (9) and applying Eq. (11) in Eq. (10), Eq. (9) gives Eq. (2).

III. FURTHER COMMENTS

It is worth comparing $D(E)$ in Eq. (6) and $D_\omega(E)$ in Eq. (8) in the complex E plane. $1/D(E)$ has a branch cut—known as the unitary cut—on the positive real axis due to the $-ip^{2\ell+1}$ term, which changes into a series of poles—called "unitary" poles below—for $1/D_\omega(E)$ [from the term $[\Sigma_\omega(E) - \mathscr{P}\Sigma(E)]/\mathscr{A}_\ell$]. Both nonanalyticities are directly connected to unitarity and thus independent of framework, power counting, and fine tuning.

However, fine tuning and power counting do impact the behavior of the ERE function [27]: in a natural case, $C_{0,j} \sim M_H^{2\ell+1-2j}$; in a first fine-tuned case, $C_{0,0}$ is enhanced; and in a second fine-tuned case, the function has low-energy poles. Note that Ref. [27] uses EFTs *without* a dimer field, and the Lagrangian is the same for the three cases, except power countings. One can add the couplings between $\mathscr{B}(x)$ and particles to the Lagrangian, again by multiplying the short-

distance-interaction terms with powers of $\boldsymbol{\partial}^2\mathscr{B}$, e.g., for s wave $\mathscr{L}_I = [\tilde{d}_0 + \sum_{k\geqslant 1}\tilde{d}_{0,k}(M_{\rm R}^2\boldsymbol{\partial}^2\mathscr{B}/3m)^k](c\,n)^*(c\,n) + \cdots$.

For each of these cases, the T matrix in a trap can be computed in the same way as the free-space one [27] but with the bare couplings substituted by the corresponding modified ones—e.g., $\tilde{d}_0 \to \tilde{d}_0 + \sum_{k\geqslant 1}\tilde{d}_{0,k}(M_{\rm R}\omega)^{2k}$—and the unitary cut by the "unitary" poles. Since the EFT calculations reproduce the free-space T matrix using ERE parameters $C_{i=0,j}$, the T matrix in a trap can be parametrized in the same way but with ω-dependent ERE parameters. The relation between these ERE parameters and the bare couplings is nonlinear, but the former's ω dependence could be expanded in terms of ω^2. (This expansion must be examined with care, if its convergence radius is much smaller than the naive estimate based on M_H, e.g., due to fine tuning of the trap's modification to the interaction at short distance.) Finally, by identifying the poles of the trap T matrix, one then reproduces Eq. (2) for the natural and the first fine-tuned case; for the second fine-tuned case, a Laurent expansion of $p^{2\ell+1}\cot\delta_\ell$ was derived [27], so the same expansion should be used on the LHS of Eq. (2) with the parameters carrying ω^2 corrections. In other words, in my approach *with* a dimer field, resumming of $d_j^{(\ell)}$ and $d_{j,k}^{(\ell)}$ terms is needed.

IV. SUMMARY

I have applied pionless EFT to two short-range interacting particles in an external harmonic trap to derive a systematically improved BERW formula that is exact even at finite ω. It is valid when the infrared scale of the trap ($\sqrt{M_{\rm R}\omega}$) and the relative momentum p are both smaller than the high-momentum scale set by the dynamics. This provides a firm foundation for implementing a Luscher-formula–like approach to connect nuclear scattering and *ab initio* structure calculations. The derivation involved new coupling terms between the background field and particles, which lead to the improvements of the original BERW formula. Moreover, a careful analysis of renormalization shows a nontrivial relation between the cutoff Λ on relative momentum in free space and cutoff n_Λ on the number of radial excitations in a trap. The renormalization procedure is further confirmed by the proof of Eq. (11). Both aspects are instructive for deducing connections between a trapped system (with two or more clusters) and free-space scattering and reactions for both nuclear and cold atom physics [20]. It should also be interesting to apply this framework to study exotic atoms[1] and quantum dots [40].

ACKNOWLEDGMENTS

I would like to thank Dick Furnstahl, Chan Gwak, Jason Holt, David Kaplan, Ubirajara Van Kolck, Petr Navratil, Daniel Phillips, Martin Savage, Ragnar Stroberg, and Chieh-Jen Yang for helpful discussions, and Yuri Kovchegov for pointing out how to use contour integration to prove Eq. (11). I also thank Dick Furnstahl and Jordan Melendez for careful proofreading of the paper. The work was supported by the National Science Foundation under Grant No. PHY-1614460 and the NUCLEI SciDAC Collaboration under US Department of Energy MSU subcontract RC107839-OSU, the US Department of Energy under contract DE-FG02-97ER-41014, and the US Institute for Nuclear Theory.

[1]Here the long-range interaction is the attractive Coulomb force. The so-called Deser-Trueman formula [40] relates the energy levels of exotic atoms to the scattering length of the short-distance interaction.

[1] C. Barbieri and A. Carbone, Lect. Notes Phys. **936**, 571 (2017).
[2] B. R. Barrett, P. Navratil, and J. P. Vary, Prog. Part. Nucl. Phys. **69**, 131 (2013).
[3] J. Carlson, S. Gandolfi, F. Pederiva, S. C. Pieper, R. Schiavilla, K. E. Schmidt, and R. B. Wiringa, Rev. Mod. Phys. **87**, 1067 (2015).
[4] D. Lee, Prog. Part. Nucl. Phys. **63**, 117 (2009).
[5] S. R. Stroberg, S. K. Bogner, H. Hergert, and J. D. Holt, Annu. Rev. Nucl. Part. Sci. **69**, 307 (2019).
[6] J. Preskill, Quantum **2**, 79 (2018).
[7] K. M. Nollett, S. C. Pieper, R. B. Wiringa, J. Carlson, and G. M. Hale, Phys. Rev. Lett. **99**, 022502 (2007).
[8] P. Navrátil, S. Quaglioni, G. Hupin, C. Romero-Redondo, and A. Calci, Phys. Scr. **91**, 053002 (2016).
[9] S. Elhatisari, D. Lee, G. Rupak, E. Epelbaum, H. Krebs, T. A. Lähde, T. Luu, and U.-G. Meißner, Nature (London) **528**, 111 (2015).
[10] A. M. Shirokov, A. I. Mazur, I. A. Mazur, E. A. Mazur, I. J. Shin, Y. Kim, L. D. Blokhintsev, and J. P. Vary, Phys. Rev. C **98**, 044624 (2018).
[11] T. Busch, B.-G. Englert, K. Rzażewski, and M. Wilkens, Found. Phys. **28**, 549 (1998).
[12] D. Blume and C. H. Greene, Phys. Rev. A **65**, 043613 (2002).
[13] M. Block and M. Holthaus, Phys. Rev. A **65**, 052102 (2002).
[14] E. L. Bolda, E. Tiesinga, and P. S. Julienne, Phys. Rev. A **66**, 013403 (2002).
[15] Z. Idziaszek and T. Calarco, Phys. Rev. Lett. **96**, 013201 (2006).
[16] I. Stetcu, B. R. Barrett, U. van Kolck, and J. P. Vary, Phys. Rev. A **76**, 063613 (2007).
[17] A. Suzuki, Y. Liang, and R. K. Bhaduri, Phys. Rev. A **80**, 033601 (2009).
[18] I. Stetcu, J. Rotureau, B. R. Barrett, and U. van Kolck, Ann. Phys. (NY) **325**, 1644 (2010).
[19] J. Rotureau, I. Stetcu, B. R. Barrett, M. C. Birse, and U. van Kolck, Phys. Rev. A **82**, 032711 (2010).
[20] D. Blume, Rep. Prog. Phys. **75**, 046401 (2012).
[21] T. Luu, M. J. Savage, A. Schwenk, and J. P. Vary, Phys. Rev. C **82**, 034003 (2010).
[22] M. Luscher, Nucl. Phys. B **354**, 531 (1991).

[23] S. R. Beane, P. F. Bedaque, A. Parreno, and M. J. Savage, Phys. Lett. B **585**, 106 (2004).
[24] J. Rotureau, I. Stetcu, B. R. Barrett, and U. van Kolck, Phys. Rev. C **85**, 034003 (2012).
[25] S. Ali, A. A. Z. Ahmad, and N. Ferdous, Rev. Mod. Phys. **57**, 923 (1985).
[26] See Supplemental Material at http://link.aps.org/supplemental/10.1103/PhysRevC.101.051602 for studies of two different toy models, details for the EFT derivation, and a proof Eq. (11), which includes Refs. [40–47].
[27] U. van Kolck, Nucl. Phys. A **645**, 273 (1999).
[28] P. F. Bedaque and U. van Kolck, Annu. Rev. Nucl. Part. Sci. **52**, 339 (2002).
[29] H. W. Hammer, C. Ji, and D. R. Phillips, J. Phys. G **44**, 103002 (2017).
[30] R. A. Briceno, Z. Davoudi, and T. C. Luu, Phys. Rev. D **88**, 034502 (2013).
[31] X. Zhang, K. M. Nollett, and D. R. Phillips, Phys. Rev. C **98**, 034616 (2018).
[32] D. B. Kaplan, M. J. Savage, and M. B. Wise, Phys. Lett. B **424**, 390 (1998).
[33] S. R. Beane and M. J. Savage, Nucl. Phys. A **694**, 511 (2001).
[34] P. F. Bedaque, H. W. Hammer, and U. van Kolck, Phys. Lett. B **569**, 159 (2003).
[35] E. Braaten and H.-W. Hammer, Phys. Rep. **428**, 259 (2006).
[36] E. Braaten, Phys. Rev. D **91**, 114007 (2015).
[37] M. A. Caprio, P. Maris, and J. P. Vary, Phys. Rev. C **86**, 034312 (2012).
[38] S. Coleman, J. Wess, and B. Zumino, Phys. Rev. **177**, 2239 (1969).
[39] D. B. Kaplan, M. J. Savage, and M. B. Wise, Nucl. Phys. B **534**, 329 (1998).
[40] M. Combescure, A. Khare, A. Raina, J.-M. Richard, and C. Weydert, Int. J. Mod. Phys. B **21**, 3765 (2007).
[41] M. Abramowitz and I. Stegun, *Handbook of Mathematical Functions* (Dover Publications, New York, 1972).
[42] R. Furnstahl, D. Phillips, and S. Wesolowski, J. Phys. G **42**, 034028 (2015).
[43] M. Petkovšek, H. S. Wilf, and D. Zeilberger, *A=B* (A K Peters, Wellesley, 1996), p. 38.
[44] DLMF, *NIST Digital Library of Mathematical Functions*, http://dlmf.nist.gov/, Release 1.0.22 of 2019-03-15, edited by F. W. J. Olver, A. B. Olde Daalhuis, D. W. Lozier, B. I. Schneider, R. F. Boisvert, C. W. Clark, B. R. Miller, and B. V. Saunders.
[45] N. M. Temme, *Special Functions: An Introduction to the Classical Functions of Mathematical Physics* (Wiley, New York, 1996).
[46] C. J. Joachain, *Quantum Collision Theory* (North-Holland, Amsterdam, 1975).
[47] M. Goldberger and K. Watson, *Collision Theory* (Wiley, New York, 1964).